J. MATER. CHEM., 1991, 1(5), 819–826

Docosanoyl Itaconate/1-Docosylamine Alternate-layer Langmuir–Blodgett Films: Polymerisation, Pyroelectric Properties and Infrared Spectroscopic Studies

John Tsibouklis,[ab] Michael Petty,[ab] Yi-Ping Song,[ac] Robert Richardson,[d] Jack Yarwood,[c] Michael C. Petty[a*] and W. James Feast[b]

[a] *Molecular Electronics Research Group, School of Engineering and Applied Science, University of Durham, South Road, Durham DH1 3LE, UK*

[b] *IRC in Polymer Science and Technology, University of Durham, South Road, Durham DH1 3LE, UK*

[c] *Department of Chemistry, University of Durham, South Road, Durham DH1 3LE, UK*

[d] *School of Chemistry, University of Bristol, Cantock's Close, Bristol BS8 1TS, UK*

Langmuir–Blodgett multilayers of an isomeric mixture of an itaconate monoester have been prepared. Multilayers were polymerised *via* initiation by irradiation with ultraviolet light and the reactions studied by UV–VIS spectrophotometry and gel permeation chromatography. Alternate-layer structures of the itaconate monomer and the corresponding polymer with an aliphatic amine have also been built-up. X-Ray reflectivity experiments have indicated that the bilayer spacing of these films did not change upon polymerisation. An evaluation of the pyroelectric properties of the alternate-layer structures revealed that, although the monomer/amine system possessed a pyroelectric coefficient of 1.4 μC m^{-2} K^{-1}, polymer/amine films were not pyroelectric. The mechanism responsible for the loss of the pyroelectric activity is discussed on the basis of infrared spectroscopic investigations.

Keywords: *Langmuir–Blodgett Film*; *Pyroelectricity*; *Solid-state polymerisation*; *Infrared spectroscopy*

It is now well established that the spontaneous electrical polarisation of certain alternate-layer Langmuir–Blodgett (LB) films is temperature dependent; such films exhibit pyroelectricity.[1–4] However, the utilisation of these films in real applications is hindered by their low stability against most solvents, mechanical stress and ageing. This lack of stability can be overcome in favourable cases by the polymerisation of reactive groups within the amphiphiles or by exploiting preformed amphiphilic polymers.[5–8]

Laschewsky *et al.*[9] have investigated a number of amphiphilic carboxylic acid derivatives capable of undergoing polymerisation in their LB form. One of the materials investigated was octadecanoyl itaconate. This compound was synthesized by the reaction of itaconic anhydride with octadecan-1-ol in toluene in the presence of zinc(II) chloride. The material formed condensed, stable monolayers which were deposited onto a hydrophilic substrate in a Y-type mode. The multilayers were polymerised on irradiation with UV light.

In this work we report the synthesis, polymerisation and LB forming characteristics of an isomeric mixture of another itaconate monoester which may be used as an active component in pyroelectric acid/amine[10] LB multilayers.

Experimental

Synthesis

The monomer mixture (**M1** and **M2**) was synthesized according to the scheme shown in Fig. 1. Bulk polymerisation of the mixture initiated by azobisisobutyronitrile (AIBN) yielded the copolymer (**P**) with repeat units **P1** and **P2** derived from monomers **M1** and **M2** respectively.

Synthesis of **M1** *and* **M2**

Two drops of concentrated sulphuric acid were added to a mixture of itaconic acid (6.505 g, 0.05 mol) and docosan-1-ol (16.330 g, 0.05 mol) suspended in dry toluene (200 cm^3) in a 500 cm^3 round-bottomed flask equipped with a Dean and

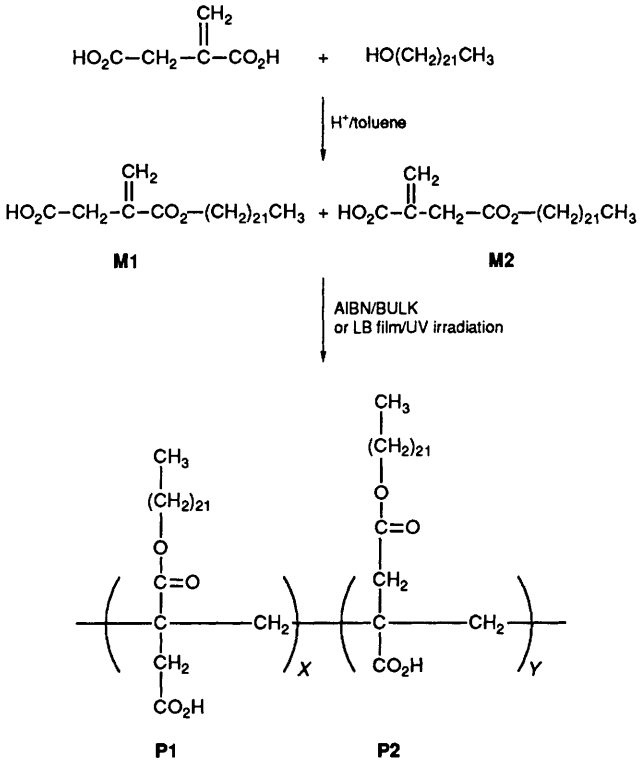

Fig. 1 Reaction scheme for the synthesis and polymerisation of **M**

Stark trap. The mixture was refluxed for 24 h. On cooling the sample, a white precipitate formed which was recovered by filtration and recrystallised twice from warm (45 °C) toluene to give (14.9 g, 0.03 mol, 60%) of monomer mixture (**M**) as a white solid, m.p. 97 °C (Found C, 73.67; H, 11.70 M^+ 439. $C_{27}H_{50}O_4$ requires C, 73.92; H, 11.50%; *M*, 439). ν_{max}/cm^{-1} 1632 (C=CH_2). δ_H (400 MHz; solvent $CDCl_3$; standard TMS)

6.46, and 5.83 (**M2**) and 6.32, 5.69 (**M1**); two pairs of vinylic protons in a ratio 85:15. There was partial resolution of the multiplet due to $-OCH_2$ at 4.10 but all the other resonances of **M1** and **M2** overlapped. Shifts and integrations were consistent with the above assignment, with allylic CH_2 at 3.34, OCH_2CH_2 at 1.61, side-chain CH_2 at 1.26 and chain-end methyl at 0.88 ppm; δ_c (300 MHz) 173.0 (s, C=O); 171.9 (s, conj. C=O); 134.3 (s, $=CH_2$); 133.4 (s, =C); 65.8 (s,$-O-CH_2-$); 36.0–25.0 (m, $-CH_2-$); 15.1 (s,$-CH_3$).

Synthesis of **P**

The monomer mixture (1 g, 2×10^{-3} mol) and AIBN (0.02 g, 1×10^{-4} mol) were mixed thoroughly and melted (88 °C/2×10^{-2} Pa) and the reaction vessel was sealed and kept at 88 °C for 2 h. The cooled mixture was dissolved in warm (50 °C) xylene (50 cm^3), precipitated with methanol (5 cm^3) and dried *in vacuo* (50 °C, 5 h) to give (0.78 g, 78%) of polymer (**P**) as a white solid which gave a mobile fluid at $T>120$ °C [Found: C, 73.44; H, 11.94. $(C_{27}H_{50}O_4)_n$ requires C, 73.92; H, 11.50%]. M_n [GPC; polystyrene standards; tetrahydrofuran (1 cm^3 min^{-1}); room temperature], 7700, bimodal, PDI: 2.39; δ_H (400 MHz; solvent acetone; standard TMS) 4.59 (b, $-O-CH_2$), 3.80 [s, $-CH_2-$ (**P1**)], 3.79 [s, $-CH_2-$ (**P2**)], 2.11 (b, OCH_2CH_2), 1.77 (b, $-CH_2-$), 1.36 (b,$-CH_3$); δ_C (300 MHz); 181.7 (b, $-CO_2-$), 171.0 (b, $-CO_2H$), 65.2 (s, $-O-CH_2-$), 46.8 (s, quat. C), 33.2 (b, $-CH_2-$), 14.7 (s, $-CH_3$).

Film Deposition and Characterisation

Monolayer studies were undertaken using a constant-perimeter barrier trough which has been described previously.[11] LB films were deposited on an alternate-layer constant-perimeter trough. Transfer of the substrate from one compartment to the other was facilitated by a gate mechanism similar to that described by Daniel *et al.*[12] The materials were spread from solutions (*ca.* 1 mg cm^{-3}) in chloroform (Aristar grade) onto water subphases at 20±1 °C. The water was purified by reverse osmosis followed by deionisation and UV sterilisation. During the measurement of isotherms and monolayer deposition, the water pH was 5.6–5.8. Monolayers were compressed to a surface pressure of 30 mN m^{-1} for deposition.

The X-ray diffraction measurements were carried out at the University of Bristol using a wavelength of 0.154 nm. A previously described, purpose-built X-ray diffractometer was used.[13]

For electrical measurements, films were deposited onto aluminised glass slides and aluminium top electrodes (30 nm thick) were evaporated. All measurements were made on samples held under vacuum. Pyroelectric coefficients were determined using a quasi-static technique.[2] The temperature of the sample was varied linearly by ±1 °C about a mean temperature of 20 °C. Relative permittivity (ε_r) and dielectric loss (tan δ) data were recorded using a Hewlett-Packard 4192A LF impedance analyser.

Polymerisation of Multilayers

The itaconate monoester was polymerised in multilayers by UV irradiation (GP Industrial Electronics, EPROM eraser UV141) under a nitrogen atmosphere. The temperature of the sample was not allowed to exceed 28 °C during the irradiation experiments.

Infrared Characterisation

For attenuated total reflection (ATR), a hydrophobic ZnSe crystal was used as a substrate and alternate-layer acid–amine LB films were obtained with a structure AABABA..., where A represents an acid molecular layer and B represents an amine molecular layer. The first two acid layers were deposited on the hydrophobic surface of the ZnSe crystal in order to aid the adhesion of the first amine layer. For RAIRS, hydrophilic aluminised glass slides were used as substrates and alternate-layer films were deposited with a structure ABABA.... A large number of layers (28 for ATR samples and 37 for RAIRS samples) were deposited on the substrates in order to minimize the effects of absorption in the first bilayer of the ATR samples and the first layer of the RAIRS samples; this can be somewhat different from the absorption in the bulk of the LB films.[14,15] The FTIR spectra were recorded on a Mattson Sirius 100 instrument at a resolution of 4 cm^{-1}. In recording RAIRS spectra, a lithographic grid polarizer (KRS-5) was used to transmit only p-polarized light.[16]

Results and Discussion

Monomer and Polymer Synthesis

The monomer mixture was synthesized by the acid-catalysed esterification of itaconic acid with docosan-1-ol. ^1H NMR investigations demonstrated that the esterification reaction produced a 85:15 molar mixture of the two possible isomers, **M2** and **M1**. No attempt was made to separate the isomers.

An attempted esterification of itaconic anhydride with docosan-1-ol in the presence of a nucleophilic base such as pyridine or 4-pyrrolidinopyridine resulted in the formation of a black tar.

The radical polymerisation of the isomer mixture was carried out in the bulk with AIBN as initiator. Gel permeation chromatography (GPC) experiments revealed that the polymer has a number-average molecular weight of *ca.* 7700, the GPC chromatogram was bimodal.

The infrared spectrum of the polymer as compared with that of the monomer is characterised by the broadening of most of the peaks and the disappearance of the double-bond absorption band, ν(C=C), at 1632 cm^{-1}. The ^1H NMR spectrum of the polymer differs from that of the monomer in that the vinylic resonances disappear and the other peaks become broader The backbone methylene is masked by the broad, aliphatic side-chain resonance at 1.77 ppm. The main feature of the polymer ^{13}C NMR spectrum as compared with that of the monomer is the disappearance of the vinylic resonances at 134.3 and 133.4 ppm, and the appearance of a new resonance at 46.8 ppm due to the quaternary carbon of the polymer backbone.

Thermogravimetric analysis results showed that the monomer was stable up to temperatures of *ca.* 270 °C whereas the polymer began to degrade at *ca.* 220 °C. These findings are indicative of a polymer degradation process associated with the backbone rather than the actual substituents on the monomer unit.

Film Formation and Polymerisation

The preformed polymer formed stable monolayers at the air/water interface (collapse rate: 2.6% h^{-1} at 30 mN m^{-1}). Fig. 2(*a*) shows the surface pressure *vs.* area per molecule isotherm for **P** (compression rate: 1 cm^2 s^{-1}, maximum area: 514 cm^2). The area per monomer unit, as estimated by extrapolating the condensed-phase region to zero pressure was 28.0±0.6 $Å^2$. Unfortunately, attempts to deposit **P** on a variety of hydrophilic or hydrophobic substrates proved unsuccessful. In order to assess the rigidity of the film, a portion of the floating monolayer (held at constant pressure)

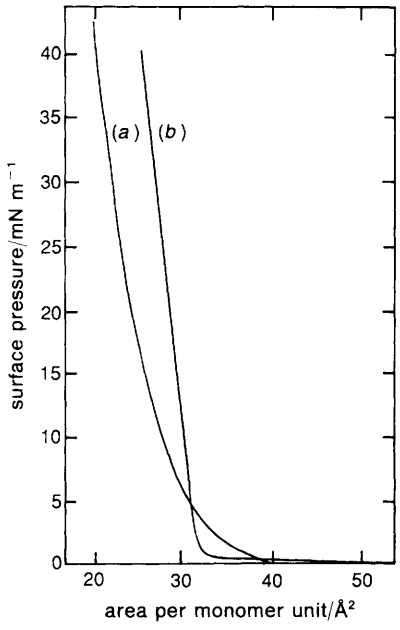

Fig. 2 Pressure *vs.* area isotherm, (*a*) **P**, (*b*) **M**

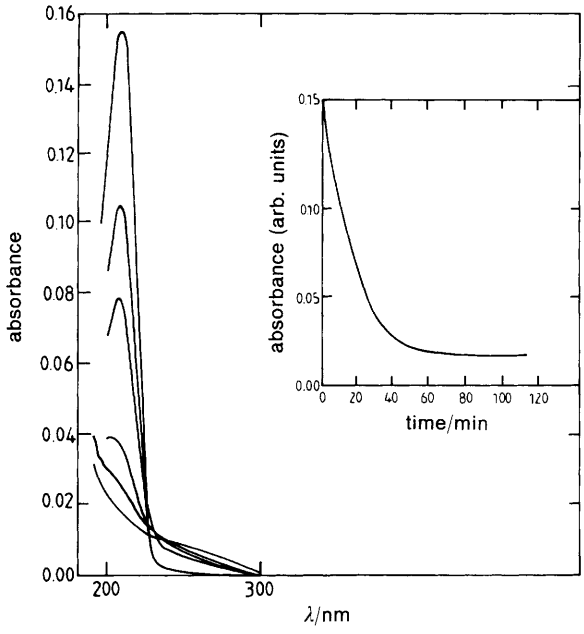

Fig. 3 UV–VIS spectra of monomer (Y-type LB film) as a function of irradiation time. Inset shows the absorbance at 207 nm as a function of irradiation time

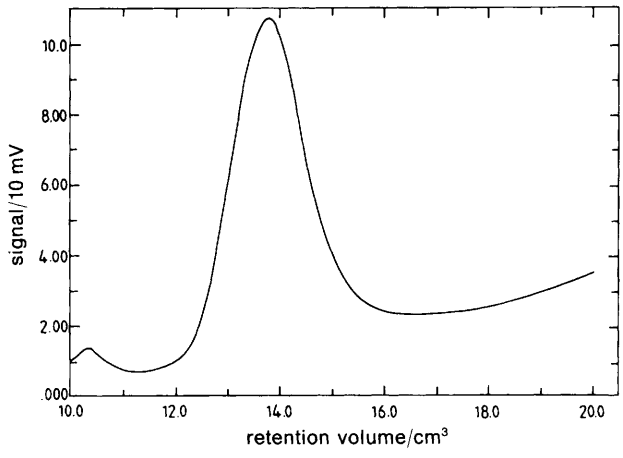

Fig. 4 Molecular-weight distribution (GPC trace) for monomer LB films polymerised by UV irradiation for 120 min

at a distance from the surfce pressure sensor was removed using a suction tube. No movement of the trough barriers was observed, indicating that the film was rigid enough to accommodate large holes.

The isotherm for the monomer mixture is shown in Fig. 2(*b*); this yielded an area per molecule of 32.0 ± 0.6 Å^2. The collapse rate was found to be 1.4% h^{-1} at 30 mN m^{-1}. Film transfer from the water surface to a variety of hydrophilic substrates (dipping speed $\leqslant 22$ mm min^{-1}) could be readily effected for the monomer mixture. The material exhibited Y-type deposition over the thickness range investigated (1–60 layers) with a transfer ratio of 1.0 ± 0.1.

To investigate the ability of monomer films to undergo polymerisation in the solid state (Fig. 1), the LB multilayers were irradiated with UV light and the reaction was followed by UV–VIS spectrophotometry; the results are shown in Fig. 3. The monomer mixture exhibits a single absorption band at 207 nm which decreases in intensity on UV irradiation. This band is attributed to the π–π^* transition of the reactive vinylic bond. Irradiation beyond 114 min led to no further loss in absorbance.

The formation of a polymer was confirmed by GPC. Photopolymerised films of the monomer mixture were washed with tetrahydrofuran, the solution was concentrated to 0.1 cm^3 and the molecular-weight distribution was determined by GPC using a VISCOTEK instrument equipped with a viscometric detector. The chromatogram is shown in Fig. 4. The drift in the baseline is due to the high sensitivity setting in the detector. A number average molecular weight of *ca.* 110 000 was obtained. The chromatogram was compared with that obtained from a sample of pure monomer; no evidence for the presence of unreacted monomer could be found. This was confirmed by comparing the GPC of the fully photopolymerised material with that of a sample partially polymerised (by masking areas of the slide from the UV source); in the latter case a monomer peak was clearly identified.

In order to form pyroelectric LB films, both the monomer and the polymer were alternated with 1-docosylamine. Again it was found that the preformed polymer could not be deposited successfully. High-quality LB multilayer films were, however, obtained by alternating the monomer mixture with 1-docosylamine, provided that the acid was deposited first on the initial upstroke.[17] These films exhibited an absorption maximum at 201 nm. The decrease in intensity as a function of irradiation time is given in Fig. 5. Following irradiation of the sample, the residual absorbance was *ca.* 50% of that observed in the original, unpolymerised sample. This does not, however, indicate that polymerisation has taken place to the extent of 50%, as there may have been contributions from other optical transitions in the same region. The GPC from an alternate-layer film, treated in the same manner as the Y-type films of the pure acid, is given in Fig. 6. It is evident that conversion to the polymer does not proceed to completion. Furthermore, the molecular-weight distribution differs considerably. This may be explained in terms of the strong head-to-head interactions between the acid and amine groups which probably induce strain and hence disrupt the molecular packing requirements for this solid-state reaction.

The thickness of the alternate-layer films deposited onto silicon wafers was measured, before and after polymerisation, using an ellipsometer (Rudolph Research, Auto EL-III; $\lambda =$ 633 nm). The experiments demonstrated that the overall thick-

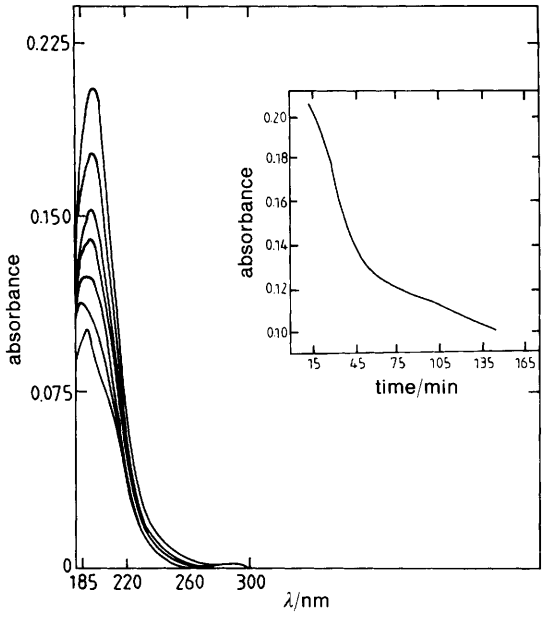

Fig. 5 UV–VIS spectra of monomer/1-docosylamine (alternate-layer LB film) as a function of irradiation time. Inset shows the absorbance at 201 nm as a function of irradiation time

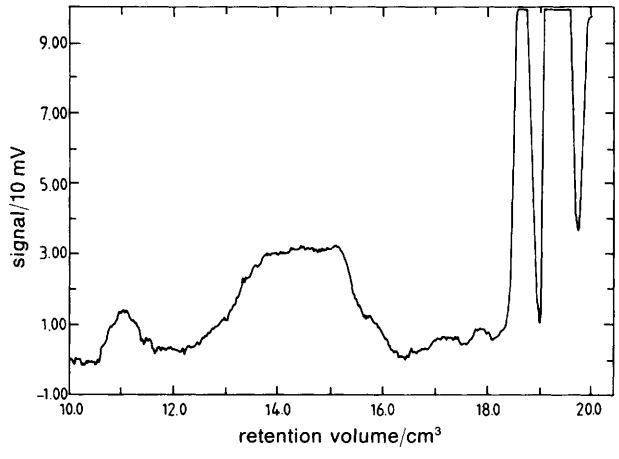

Fig. 6 Molecular-weight distribution (GPC trace) for monomer/1-docosylamine films polymerised by UV irradiation for 180 min

ness (6.3 ± 0.1 nm per bilayer) of the alternate-layer film did not change upon polymerisation. This was further confirmed by low-angle X-ray reflectivity measurements. The reflectivity profiles for unpolymerised and polymerised films are shown in Fig. 7. In both cases the *d*-spacing (bilayer spacing) was calculated to be 6.0 ± 0.02 nm using the Bragg law. The sum of the molecular lengths, measured using a CPK space-filling model, was of the order of 6.6 nm. Assuming no interdigitation, an average tilt angle of 24° with respect to the substrate normal was calculated. The similarity between the two reflectivity profiles indicates that polymerisation does not significantly change the inter-layer spacing of these films.

Dielectric and Pyroelectric Characterisation

The mode of operation of a typical pyroelectric device relies upon the measurement of potential difference across a pyroelectric element upon which chopped radiation is imaged. In this case the efficiency of signal extraction is influenced by the capacitance of the detector. Thus a useful figure of merit,

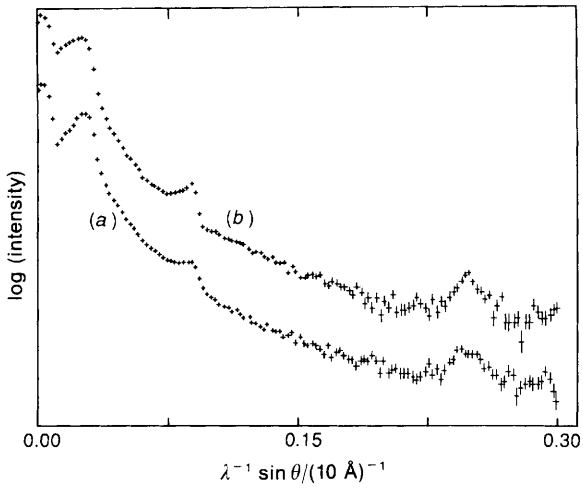

Fig. 7 X-Ray reflectivity profiles of monomer/1-docosylamine alternate layer films: (*a*) unpolymerised; (*b*) polymerised. Curve (*b*) has been displaced vertically for clarity

F_V, is defined as:[18]

$$F_V = p/\varepsilon_r$$

where p is the pyroelectric coefficient. Also, if the dielectric loss should become large, this will further hinder the performance of the device and a slightly different figure of merit, F_D, becomes appropriate where,

$$F_D = p/\sqrt{(\varepsilon_r \tan \delta)}$$

The relative permittivity and dielectric-loss data for unpolymerised and polymerised alternate layer films are shown in Fig. 8(*a*) and (*b*), respectively. The data were measured over the frequency range 10–100 kHz and have been corrected for lead resistance. As can be seen from Fig. 8, the relative permittivity and dielectric loss of both film types are of low value and are frequency independent in the range studied. Unpolymerised alternate-layer films displayed a pyroelectric signal of 1.4 ± 0.1 μC m^{-2} K^{-1}, which is comparable with that of the well studied, simple acid/amine systems.[2,4,11] The average relative permittivity and dielectric loss of the unpolymerised film in the frequency range studied was 2.60 and 0.002, respectively. These data yield $F_V = 0.54$ μC m^{-2} K^{-1} and $F_D = 19.4$ μC m^{-2} K^{-1} which compare favourably with

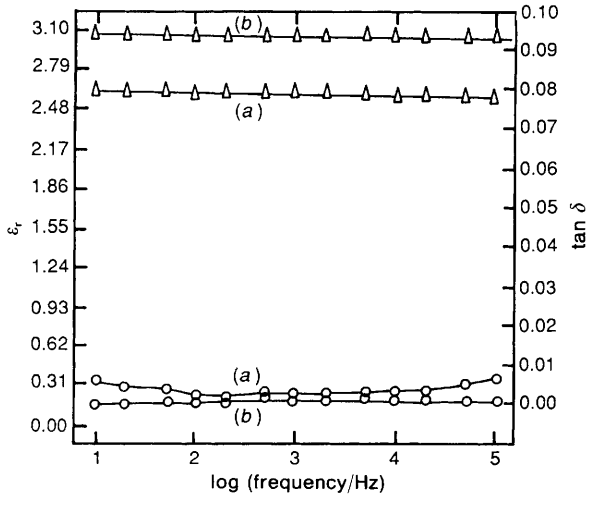

Fig. 8 Relative permittivity (△) and dielectric loss (○) data of monomer/1-docosylamine alternate-layer films: (*a*) unpolymerised; (*b*) polymerised

those of PVDF ($F_V = 2.3\ \mu C\ m^{-2}\ K^{-1}$ and $F_D = 63.6\ \mu C\ m^{-2}\ K^{-1}$).[18] The dielectric losses of the LB structures are typically an order of magnitude lower than those of PVDF and, hence, the former figure of merit may be more appropriate. No pyroelectric signals could be detected for the alternate-layer films after polymerisation.

Previous workers have attributed the origin of the pyroelectric effect in LB films to changes in molecular volume,[4] molecular orientation[19] and the degree of proton transfer[17] upon heating/cooling. The loss of pyroelectric activity after UV irradiation indicates that the pyro-mechanism is affected by either the polymerisation itself, photochemical degradation or a structural rearrangement such that the non-centrosymmetric nature of the film is lost. The results of our X-ray investigations would appear to eliminate the last possibility. Since the polymerisation in the itaconate monoester molecules occurs close to the polar headgroups, the reduced freedom of motion near the supposed active site of the molecules may prevent the lateral expansion and/or tilting of the dipoles in the film. In addition, the polymerisation may affect the nature of any proton transfer occurring between the acid and amine molecules due to the proximity of the vinylic bond to the carboxylate group. In order to investigate the detailed molecular arrangements in both the unpolymerised and polymerised alternate-layer films and to elucidate the mechanism responsible for their pyroelectric behaviour a series of FTIR experiments was performed.

Infrared Analysis

We first discuss the IR spectrum of the monomer mixture, then that of the alternate-layer LB films and finally that of the polymerised film.

Cast-film Spectra of the Acid Mixture

The transmission–absorption spectrum of a cast film of the acid mixture on a ZnSe crystal is shown in Fig. 9. The assignments of the principal bands are listed in Table 1. Each chemical group is discussed separately.

Ethylenic Group Absorption. The ethylenic ν(C=C) mode in a structure of $R_1R_2C{=}CH_2$ typically absorbs near 1653 cm^{-1}.[20] Conjugation of the double bond results in a shift to lower frequency. For these molecules the ethylenic bond is either conjugated with the ester carbonyl or the acid carbonyl bonds and therefore the 1638 cm^{-1} band can be attributed to the ν(C=C) mode. The CH_2 out-of-plane deformation in $R_1R_2C{=}CH_2$ typically absorbs at 890 cm^{-1}.[20] Since carbonyl groups attached directly to the double bond raise the frequency to 930–945 cm^{-1},[20] the 943 cm^{-1} band can be attributed to this mode. The planar deformation of the $=CH_2$ group usually absorbs in the range 1420–1410 cm^{-1} with high degree of consistency (within a few cm^{-1}). In these molecules, because of the conjugation of the double bonds with carbonyl bonds, this band is shifted down slightly to 1404 cm^{-1}.

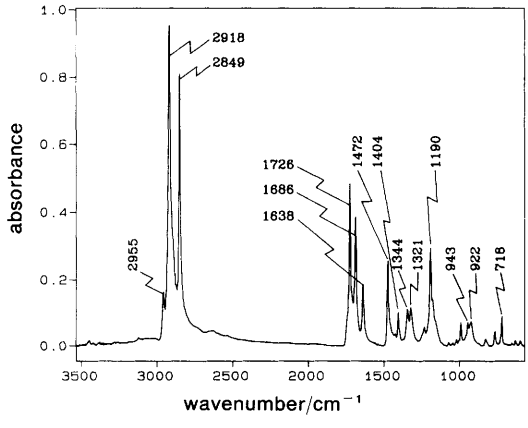

Fig. 9 Transmission spectrum of a cast film of the docosanoyl itaconate monomer mixture

Table 1 Band position and assignments for the cast film of the docosyl itaconate

ν_{max}/cm^{-1}	assignment	comments
2955	$\nu_{as}(CH_3)$	antisymmetric stretch
2918	$\nu_{as}(CH_2)$	antisymmetric stretch
2849	$\nu_s(CH_2)$	symmetric stretch
1726	ν(C=O)	ester group
1686	ν(C=O)	conjugated acid dimer (**M2**)
1638	ν(C=C)	ethylenic
1472	$\delta(CH_2)$	scissoring
1404	$b_{ip}(=CH_2)$	$=CH_2$ in-plane deformation
1344	ν(CC) (**M1**)	with double-bond character
1321	ν(CC) (**M2**)	with double-bond character
1190	ν(CO)	ester group
943	$b_{op}(=CH_2)$	$=CH_2$ out-of-plane deformation
922	b_{op}(OH)	OH out-of-plane deformation
718	$r(CH_2)$	alkyl-chain rocking mode

Ester Group Absorption. The ν(C=O) mode of esters typically gives rise to a band between 1748–1730 cm^{-1}. There is a small progressive fall in the frequency as the length of the alkyl chain is increased.[20] The frequency is also lowered by $\alpha\beta$ unsaturation. Therefore, the 1726 cm^{-1} band can be attributed to the ν(C=O) mode of the conjugated ester groups in **M1**. The shoulder to the higher-frequency side of this band can be attributed to the ν(C=O) mode of the unconjugated ester group in **M2**. The ν(C—O) stretching modes of esters usually give rise to strong absorption bands in the region 1300–1000 cm^{-1}. According to Bellamy,[20] if the alkyl group is longer than three carbons, which is the case here, the strongest band will be near 1190 cm^{-1}. Thus the 1190 cm^{-1} band can be attributed to the ν(CO) stretching mode.

Acid Group Absorptions. For saturated aliphatic acid dimers, the ν(C=O) mode absorbs in the region 1725–1705 cm^{-1}. For the **M2** molecule, the acid carbonyl bond is conjugated with the ethylenic bond and therefore it absorbs at 1686 cm^{-1}. Recall that the shoulder to the higher-frequency side of the 1726 cm^{-1} band was attributed to the unconjugated ester ν(C=O) of **M2**. The shoulder to the lower-frequency side of the 1726 cm^{-1} band can be attributed to ν(C=O) mode of the unconjugated acid dimer (**M1** dimer). The OH stretching mode of an acid dimer gives rise to a broad absorption region with many sub-maxima between 3000 and 2500 cm^{-1}. Thus the broad absorption in this region in Fig. 9 may be attributed to this mode. The OH deformation mode of the acid dimer usually gives rise to a broad and reasonably intense band near 935 cm^{-1}. In this case it was observed at 922 cm^{-1}.

The C—C Stretching Mode with Double-bond Character. We now draw attention to the 1344 and 1321 cm^{-1} bands. As a result of the conjugation of the ester carbonyl bond with the ethylenic double bond in **M1**, and the conjugation of the acid carbonyl bond with the ethylenic double bond in **M2**, the conjugated C—C bond has some double-bond character in both molecules. However, since the carbonyl groups in the acids are hydrogen bonded to the acid groups of other molecules, they have less double-bond character than those

in the ester groups. We may therefore assign the 1344 cm^{-1} band to the conjugated ν(CC) mode of **M1** and the 1321 cm^{-1} band to that of **M2**.

Alternate-layer LB Films

The ATR and RAIRS spectra of the alternated LB films before UV-irradiation are shown in Fig. 10. By comparing these spectra with the spectrum of the cast film, the interactions between the acid and the amine may be elucidated. In addition, comparison of the ATR and RAIRS spectra provides orientation information for the various molecular groups in the multilayer.

Molecular Interactions. When an acid is alternated with an amine in LB films, proton transfer from the acid to the amine is expected.[17] This accounts for the following changes in the spectra, on going from the cast acid film to the acid–amine LB film: (i) The most obvious change is the disappearance of the carbonyl band of the acid dimer at 1686 cm^{-1}, and the emergence of a band at 1568 cm^{-1}, due to the $\nu_{as}(CO_2^-)$ mode, and a band at 1381 cm^{-1}, due to the $\nu_s(CO_2^-)$ mode. These $\nu(CO_2^-)$ bands are not well defined. One of the reasons for this is that the $\delta(NH_3^+)$ also absorbs in this region. This band is particularly strong in RAIRS (at 1583 cm^{-1}) and therefore it may be attributed to the symmetric bending mode of the NH_3^+ group. (ii) The other important change is that the band resulting from the conjugated ν(CC) mode of **M2**, which absorbs at 1321 cm^{-1} in the cast film, disappears in both the ATR and RAIRS spectra. The acid is ionized so its carbonyl bond loses some of its double-bond character. As a result, the ν(CC) bond loses its double-bond character and its absorption shifts away from the neighbourhood of the 1321 cm^{-1} region. On going from the cast film to the LB film, the frequency of the ν(C=O) mode of **M1** increases from 1726 to 1736 cm^{-1} and the conjugated ν(CC) mode shifts down from 1344 to 1336 cm^{-1}. These shifts result from the decrease of the degree of the conjugation after the ionization of the acid.

Molecular Orientation and Arrangements. Using the method we have previously proposed,[21] the orientation of the transition dipole moments of all the IR-active vibrations of interest may be estimated. We first determine the orientation of a reference transition dipole moment, *e.g.* $\nu_{as}(CH_2)$. In order to do so, we assume that the transition dipole moment, μ_1, associated with the $\nu_{as}(CH_2)$ band at 2918 cm^{-1} is perpendicular to the transition dipole moment, μ_2, associated with the ester ν(CO) band at 1196 cm^{-1} [Fig. 11(*a*)]. From this assumption the average tilt angle of μ_1, θ_1^{av}, is defined by

$$\tan^2 \theta_1^{av} = \frac{\langle \sin^2 \theta_1 \rangle}{\langle \cos^2 \theta_1 \rangle} \quad (1)$$

[where the θ_1 is defined in Fig. 13(*a*) and the angular brackets represent an average over μ_1 of all the molecules sampled] and can be determined by[21]

$$\tan^2 \theta_1^{av} = \frac{\alpha_{ATR}(\mu_1)}{\alpha_{ATR}(\mu_2)} \frac{\alpha_R(\mu_2)}{\alpha_R(\mu_1)} \quad (2)$$

where α_{ATR} and α_R are the absorbances in ATR and RAIRS, respectively. The peak-height ratios of the $\nu_{as}(CH_2)$:ν(CO) in ATR and RAIRS are 25.8 and 1.93, respectively. Thus the average angle (θ_{ref}^{av}) of the transition dipole moments due to $\nu_{as}(CH_2)$ is calculated to be 75°. Having obtained this angle as a reference, we can now use the formula[21]

$$\cos^2 \theta^{av} = \cos^2 \theta_{ref}^{av} \frac{\alpha_{ATR}(\mu_{ref})}{\alpha_{ATR}(\mu)} \frac{\alpha_R(\mu)}{\alpha_R(\mu_{ref})} \quad (3)$$

to obtain all the other transition dipoles of interest. In eqn. (3) μ_{ref} is the transition dipole associated with $\nu_{as}(CH_2)$ vibration mode and the θ_{ref}^{av} the corresponding average tilt angle; μ is the transition dipole associated with any other vibrational mode and the θ^{av} the corresponding average tilt angle [Fig. 11(*b*)]. The results of the calculations are listed in Table 2.

Assuming the carbon chains are linear, the average direction of the chains should then be perpendicular to the average transition dipole moments of $\nu_{as}(CH_2)$, $\nu_s(CH_2)$, $\delta(CH_2)$, and r(CH_2). Thus the tilt angle of the average direction of the carbon chains is 17±2°. The deviation is estimated by assuming a 5% error in determining the band intensities.

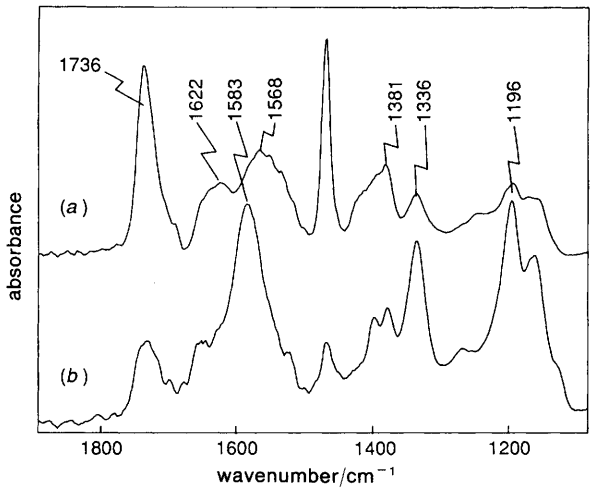

Fig. 10 ATR (*a*) and RAIRS (*b*) spectra of the alternate acid–amine LB films

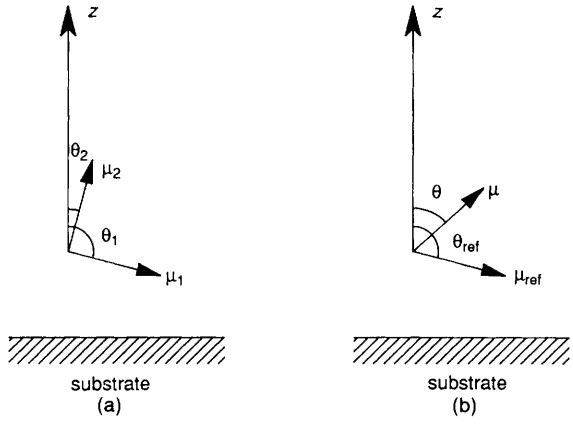

Fig. 11 Schematic representations of transition dipole moments and their tilt angles with respect to the surface normal

Table 2 Tilt angles θ of transition dipole moments in the LB film before UV irradiation

mode with which μ is associated	$\alpha_{ATR}(\mu_{ref})^a/\alpha_{ATR}(\mu)$	$\alpha_R(\mu_{ref})/\alpha_R(\mu)$	$\theta^{av}/°$ [b]
$\nu_s(CH_2)$	1.63	1.92	76 (or 104)±1.3
ester ν(C=O)	9.94	1.94	54 (or 126)±3.4
$\delta(CH_2)$	8.68	5.41	71 (or 109)±1.9
conjugated ν(CC)	29.9	2.35	23 (or 157)±5.3
ν(CO)	25.8	1.93	19 (or 161)±5.7
r(CH_2)	25.7	17.9	72 (or 108)±1.8

[a] μ_{ref} is the transition dipole moment associated with $\nu_{as}(CH_2)$ and θ_{ref} = 75°. [b] Deviations are estimated assuming a 5% error in determining the band intensities. Two values for each dipole moment are possible because of the square cosine nature of eqn. (3).

Polymerised LB Films

The ATR and RAIRS spectra of the LB films both before and after UV irradiation are shown in Fig. 12 and 13; considerable changes are evident.

Chemical Changes. The intensity of the ν(C=C) band at 1622 cm^{-1} decreases to a small proportion of its original intensity, see Fig. 12. Since this band is poorly defined, the change is difficult to determine precisely; however, curve-fitting shows that the intensity has decreased to *ca.* 16% of its original value. The band at 1336 cm^{-1} in both Fig. 12 and 13, which is attributed to the ν(CC) mode with double-bond character, has also decreased to a small proportion of its original intensity on polymerisation. Again, it is possible to evaluate the quantitative decrease by curve fitting with the result that the band is reduced to *ca.* 15% of its original intensity. It can be seen also (Fig. 12) that the out-of-plane $=CH_2$ deformation band at 945 cm^{-1} has largely disappeared. Furthermore, the shoulder to the higher-frequency side of the broad band peaked at 1381 cm^{-1} has decreased considerably in intensity. This shoulder could be attributed to the $=CH_2$ in plane deformation mode. Finally, the strongest absorption band due to the ester C—O stretches shifts down from 1196 to 1173 cm^{-1}. All these spectral changes confirm that polymerisation of the molecules in the LB films has taken place, although the process may not be complete.

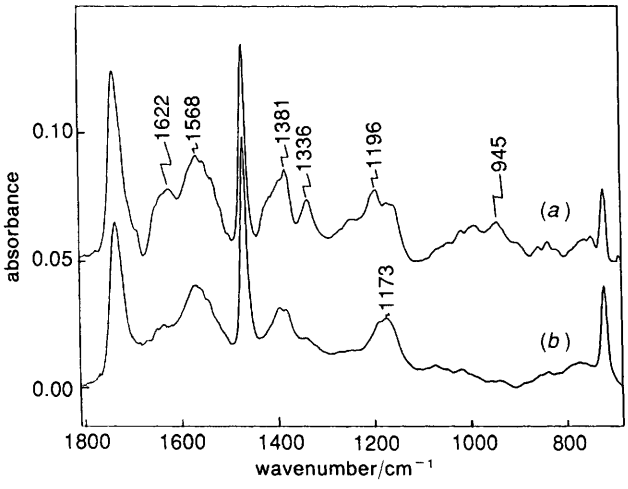

Fig. 12 ATR spectra of the LB film before (*a*) and after (*b*) UV irradiation

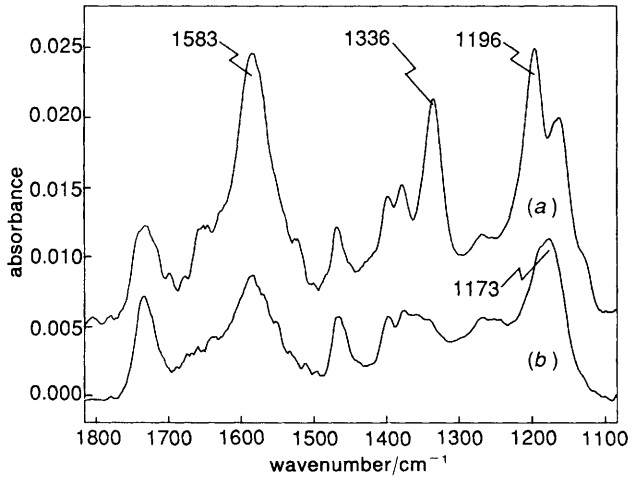

Fig. 13 RAIRS spectra of the LB film before (*a*) and after (*b*) UV irradiation

Structural Changes. Using the same algorithm (*i.e.* comparing ATR and RAIRS), we can now determine the orientation of individual dipole moments for the polymerised LB films. First, using the band-intensity ratios of $\nu_{as}(CH_2):\nu(CO)$ (26.3 and 3.15 in ATR and RAIRS) we obtain the average tilt angle of the $\nu_{as}(CH_2)$ transition dipole moment at 71°. Hence we can use eqn. (2) to determine the tilt angles for other transition dipole moments. The results are listed in Table 3. The tilt angle of the carbon chains is now $18\pm2°$. This is essentially the same as that in the unpolymerised films, since the difference is within experimental error. This result supports the hypothesis that the ordering of the alkyl chains does not change on polymerisation, in agreement with our previous X-ray reflectivity measurements. Furthermore, the band positions and the widths of the $\nu(CH_2)$ stretching bands are not changed at all on polymerisation, suggesting that no significant conformational changes or disordering occurs in the alkyl group domains of the film during polymerisation.

An interesting change in Fig. 13 is the reduction in intensity of the band at *ca.* 1583 cm^{-1} on polymerisation. We believe that the initial high intensity of this band is associated with a bending mode of the NH_3^+ group with a transition dipole perpendicular to the substrate. (Note that this composite band is shifted considerably from its position in ATR, see Fig. 12.) On polymerisation it would appear that the orientation or ordering of the NH_3^+ group is altered, possibly resulting from changes in geometry of the $-CO_2^-$ groups, and a decrease in intensity in RAIRS is induced. Unfortunately, the composite nature of this band eliminates any chance of getting quantitative intensity or geometrical information about either CO_2^- or NH_3^+ groups.

Summary of Structural Analysis Results

The results of the structural investigations are summarised as follows: (i) the multilayer structure, and in particular the bilayer spacing and molecular orientation, are unchanged by polymerisation; (ii) no photodegradation of the LB film is apparent after exposure to the UV source; and (iii) polymerisation does not appear to affect significantly proton transfer from the acid to the amine groups.

Generally, pyroelectric behaviour may originate from a primary process, *i.e.* a change in the magnitude or orientation of a dipole with temperature, or from a secondary effect *i.e.* a piezoelectrically induced change as a result of a dimensional change. It is also possible for surface and volume charges to contribute to the measured signal (tertiary or 'false' pyroelectricity). The last case may be distinguished by performing measurements after temperature cycling and/or short-circuiting the sample. From the results of such experiments on

Table 3 Tilt angles θ of transition dipole moments after UV irradiation

mode with which μ is associated	$\alpha_{ATR}(\mu_{ref})^a/\alpha_{ATR}(\mu)$	$\alpha_R(\mu_{ref})/\alpha_R(\mu)$	$\theta^{av}/°$ [b]
$\nu_s(CH_2)$	1.64	1.96	73 (or 107)±1.8
ester ν(C=O)	10.9	4.85	61 (or 119)±2.9
$\delta(CH_2)$	7.25	6.00	69 (or 111)±2.1
ν(CO)	26.3	3.14	20 (or 160)±5.6
$r(CH_2)$	18.1	28.5	75 (or 105)±1.5

[a] μ_{ref} is the transition dipole moment associated with $\nu_{as}(CH_2)$ and $\theta_{ref}=71°$. [b] Deviations are estimated assuming a 5% error in determining the band intensities.

simple acid–amine LB films, we do not believe that this is a significant process in the films under discussion in this work.[22]

We are therefore led to the conclusion that the pyroelectric activity in our molecular assemblies originates from the temperature dependence of the lateral expansion and/or tilting of the dipoles in the films. The loss of activity may then be explained in terms of the restriction of movement of the individual dipoles imposed by polymerisation. This model is in good agreement with our previous studies on the temperature dependence of pyroelectricity in simple acid/amine LB films, in which both primary and secondary processes were identified as making contributions to the pyroelectric signal.[23]

Clearly, if this is correct, there is a good reason for investigating the pyroelectric properties of a polymeric LB system in which the molecules are cross-linked at some distance from the polar heads. Such work is currently in hand.

Conclusion

An amphiphilic itaconate monoester has been synthesized and polymerised. The preformed polymer proved unsuitable for LB deposition. However, monomer multilayer structures could readily be built-up. These films polymerised upon irradiation with UV light. The monomer was alternated with 1-docosylamine to give multilayer films with a pyroelectric coefficient of 1.4 $\mu C\ m^{-2}\ K^{-1}$. The alternate-layer films were polymerised under UV irradiation and, although no change in bilayer spacing was observed, all pyroelectric activity was lost. On the basis of FTIR results we propose that the pyroelectric activity of these acid–amine LB films arises from the temperature dependence of the head group orientational and/or packing changes. The loss of the pyroelectric activity on polymerisation may therefore be the result of the increase of the molecular rigidity of the structures in the head-group region.

This work was carried out under the SERC/DTI LINK Molecular Electronics Initiative. The authors are grateful to both SERC and Thorn-EMI for support, and thank Mr. G. Forrest for performing the GPC experiments and Mr. S. Haslam for help with the X-ray measurements.

References

1 P. Christie, G. G. Roberts and M. C. Petty, *Appl. Phys. Lett.*, 1986, **48**, 1101.
2 C. A. Jones, M. C. Petty and G. G. Roberts, *Proc. 6th IEEE Int. Symp. Appl. Ferroelectrics*, IEEE, New York, 1986, p. 195.
3 G. G. Roberts, *Ferroelectrics*, 1989, **91**, 21.
4 G. W. Smith, M. F. Daniel, J. W. Barton and N. Ratcliffe, *Thin Solid Films*, 1985, **132**, 125.
5 A. Cemel, T. Fort Jr. and L. B. Lando, *J. Polym. Sci., Polym. Chem. Ed.*, 1972, **10**, 2061.
6 B. Tieke, H. J. Craf, G. Wegner, D. Naegele, H. Ringsdorf, A. Banerjie, D. Day and J. B. Lando, *Colloid Polym. Sci.*, 1977, **255**, 521.
7 R. H. Tredgold and C. Winter, *Thin Solid Films*, 1983, **99**, 81.
8 R. Elbert, A. Laschewsky and H. Ringsdorf, *J. Am. Chem. Soc.*, 1985, **107**, 4134.
9 A. Laschewsky, H. Ringsdorf and G. Schmidt, *Thin Solid Films*, 1985, **134**, 153.
10 C. A. Jones, M. C. Petty, G. G. Roberts, G. Davies, J. Yarwood, N. M. Ratcliffe and J. W. Barton, *Thin Solid Films*, 1987, **155**, 187.
11 M. C. Petty, in *Polymer Surfaces and Interfaces*, ed. W. J. Feast and H. S. Munro, Wiley, New York, 1987, p. 163.
12 M. F. Daniel, J. C. Dolphin, A. J. Grant, K. E. N. Kerr and G. W. Smith, *Thin Solid Films*, 1985, **133**, 235.
13 R. Richardson and S. J. Roser, *Liq. Cryst.*, 1987, **2**, 797.
14 Y. P. Song, J. Yarwood, J. Tsibouklis, W. J. Feast, J. Cresswell and M. C. Petty, *Langmuir*, in the press.
15 H. Ancelin, G. Briody, J. Yarwood, J. P. Lloyd, M. C. Petty, M. M. Ahmad and W. J. Feast, *Langmuir*, 1990, **6(1)**, 172.
16 Y. P. Song, M. C. Petty and J. Yarwood, *Vibrational Spectrosc.*, 1991, **1**, 305.
17 G. H. Davies, J. Yarwood, M. C. Petty and C. A. Jones, *Thin Solid Films*, 1988, **159**, 461.
18 R. W. Whatmore, *Rep. Prog. Phys.*, 1986, **49**, 1335.
19 L. M. Blinov, N. V. Dubinin, L. N. Mikhnev and S. G. Yudin, *Thin Solid Films*, 1984, **120**, 161.
20 L. J. Bellamy, *The Infrared Spectra of Complex Molecules*, Chapman and Hall, London, 3rd edn., 1986, vol. 1.
21 Y. P. Song, J. Yarwood, J. Tsibouklis, W. J. Feast and M. C. Petty, *Langmuir*, in the press.
22 C. A. Jones, M. C. Petty, G. Davies and J. Yarwood, *J. Phys. D*, 1988, **21**, 95.
23 C. A. Jones, M. C. Petty and G. G. Roberts, *Thin Solid Films*, 1988, **160**, 117.

Paper 1/01786A *Received* 17*th April*, 1991